Available online at www.sciencedirect.com

SCIENCE DIRECT®

Cement and Concrete Research 35 (2005) 473–482

CEMENT AND CONCRETE RESEARCH

Effect of fly ash on autogenous shrinkage

Pipat Termkhajornkit[a,*], Toyoharu Nawa[a], Masashi Nakai[b], Toshiki Saito[c]

[a] *Division of Structural and Geotechnical Engineering, Graduate School of Engineering, Hokkaido University, North 13 West 8, Kita-ku, Sapporo, Hokkaido 060-8628, Japan*

[b] *Department of Research and Development, Civil Engineering Section, Hokkaido Electric Power Co., Inc., 2-1, Tsuishikari, Ebetsu, Hokkaido 067-0033, Japan*

[c] *Civil Engineering Department, Hokuden-Kogyo Co., Ltd., Meijiseimei Building, 2-5, 5th Floor, N1 E1, Chuo-ku, Sapporo, Hokkaido 060-0031, Japan*

Received 23 December 2003; accepted 1 July 2004

Abstract

The correlation between autogenous shrinkage and degree of hydration of fly ash was determined with the selective dissolution method. Then, the relationship between the degree of hydration of fly ash and autogenous shrinkage was examined. The results showed that the degree of hydration of fly ash increased as its Blaine surface area increased. The degree of hydration of fly ash increased with time, and autogenous shrinkage increased corresponding to the increase in the degree of hydration of fly ash. Moreover, it was found that the total quantity of Al_2O_3 in cement–fly ash samples affected autogenous shrinkage at early ages, but the long-term influence was very small.

Keywords: Fly ash; Hydration; Ettringite; Autogenous shrinkage

1. Introduction

The recent development of certain kinds of high-performance concrete such as high-strength and self-compacting concretes tends to reduce the water-to-binder ratio and increase the paste content. These kinds of concrete show greater autogenous shrinkage than conventional concrete does, and cracks appear under certain circumstances [1–4]. One explanation is that the driving force comes from capillary tension brought about by self-desiccation in the pore structure of concrete as the moisture is consumed during the hydration process [5,6]. Cracks at early ages of conventional concrete generally occur due to improper curing and may be avoided by workmanship of good quality. However, autogenous shrinkage in high-strength concrete cannot be avoided even when there has been a good curing process [7,8].

Many previous studies showed that fly ash, as a pozzolanic material, is effective for improving the various properties of concrete. It has also been reported that damage due to autogenous shrinkage is significantly reduced in concrete or cement paste when fly ash is added [9]. However, in particular, when fly ash with a very much smaller average particle size than cement was used, larger autogenous shrinkage was found [10,11]. This implies that very small fly ash particles act like silica fume. A larger content of small particles in the paste leads to a closer distance between the particles, thereby bringing about smaller pores in the paste. Smaller pores result in a greater capillary pressure in the paste when water is consumed by the hydration of cement [10].

Many researchers have reported on the correlation between autogenous shrinkage and the degree of hydration of ordinary Portland cement (OPC; [12–15]). However, only a few papers have been issued that report on fly ash–cement mixtures.

In case of OPC, the degree of hydration can be measured by many methods such as nonevaporate water content,

---

[*] Corresponding author. Tel.: +81 11 706 6306.
E-mail address: tpipat@eng.hokudai.ac.jp (P. Termkhajornkit).

0008-8846/$ - see front matter © 2004 Elsevier Ltd. All rights reserved.
doi:10.1016/j.cemconres.2004.07.010

Table 1
The physical and chemical properties of fly ash and OPC

	PR/BA	TU	CA	OPC
Ignition loss (%)	1.8	0.1	2.3	0.77
SiO_2 (%)	68.8	57.4	58.6	20.84
Al_2O_3 (%)	18.5	23.47	25.11	5.95
Fe_2O_3 (%)	3.79	7.71	5.02	2.62
CaO (%)	0.76	3.22	2.8	63.63
MgO (%)	0.46	1.25	1.13	1.79
Na_2O (%)	0.19	0.11	0.21	0.18
K_2O (%)	0.69	1.91	1.32	0.33
TiO_2 (%)	–	1.06	–	0.34
MnO (%)	–	0.12	–	0.1
Density (kg/m^3)	2130	2300	2260	3150
Bulk specific density (%)	57.3	69.1	59.5	–
Blaine surface area (m^2/kg)	279	210	426	347
Particle smaller than 45 μm (%)	21	28	12	–
C_3S	–	–	–	51.2
C_2S	–	–	–	21.2
C_3A	–	–	–	11.3
C_4AF	–	–	–	8

ignition loss of samples, X-ray diffraction and so on [12,16–18]. In the fly ash cement mixtures, the total degree of hydration can be estimated by the rate of heat evolution from the isothermal calorimeter [13,14]. However, it is not possible to measure the individual degree of hydration of fly ash using this method. In other words, this method is incapable of identifying the amount of unreacted fly ash.

In fact, fly ash, like other mineral admixtures, contributes to the properties of concrete as to both the filler effect and the pozzolanic effect [19]. In paste with a high replacement ratio of fly ash and considerably low water–binder ratio, unreacted fly ash behaves like a part of the microaggregates [16]. The problem is that methods for measuring the degree of hydration of OPC cannot be applied to measuring fly ash hydration. For example, the degree of hydration, which can be interpreted from the nonevaporate water of OPC, is reliable, based on the results of an experiment in which 1 g of anhydrous cement produced 0.23 g of nonevaporate water when it hydrated completely [20]. However, in the case of fly ash, the weight of nonevaporate water after full hydration was found to vary due to the quality of the fly ash. There were two purposes of this research: (1) to find the method for precisely determining the degree of hydration of fly ash and (2) to clarify the correlation between the degree of hydration of fly ash and autogenous shrinkage. The effect of the chemical composition of fly ash on autogenous shrinkage is also discussed.

2. Materials and methods

2.1. Materials

Ordinary Portland cement (OPC) and three kinds of fly ash were used. The chemical and physical properties of OPC and fly ash are shown in Table 1. A polycarboxylate-based superplasticizer was used as the chemical admixture.

The fly ash replacement ratios were 25 and 50 vol.% of powder. The fly ash–OPC samples were prepared with a water/powder ratio of 0.30 by weight, whereas the OPC samples were prepared with a water/powder ratio of 0.22 and 0.30 by weight. The proportion of concrete was designed to produce a diameter of slump flow of 650±50 mm, corresponding to that of self-compacting concrete. The concrete mix proportions are shown in Table 2.

To measure the degree of hydration of fly ash, paste samples were prepared with exactly the same water/powder ratio and fly ash replacement as used in the concrete test. We assumed that the degree of hydration of fly ash in the concrete is equal to that in the paste made with the same fly ash replacement and water/powder ratios.

2.2. Determination of degree of hydration of fly ash

To stop the hydration reaction, the paste samples were cracked and soaked in acetone for 1 day. These samples were dried at room temperature (20 °C) for 2 h and further dried at 40 °C for 3 h. Then, the samples were ground until the powder passed through a 150-μm sieve. After that, the samples were dried again at 110 °C for 12 h.

The degree of hydration of fly ash was determined by a selective dissolution method. Takashima [21] reported that the unreacted fly ash in hardened fly ash–cement paste was

Table 2
Mix proportions

W/C (wt.%)	Sample	F/(C+F) (vol.%)	s/a (%)	(kg/m^3)							Slump flow diameter (mm)	Air void (%)	Temperature (°C)
				W	C	F	S	G	SP(SP8HU)				
										(C×wt.%)			
22	OPC 22	0	43	165	750	0	647	880	10.5	1.40	624	1.2	22.5
30	OPC 30	0	48.5	165	550	0	804	880	4.95	0.90	674	1.2	22
30	PR/BA 25%	25	48.5	158	431	97	804	880	4.75	(0.90)	671	1.4	20.5
30	PR/BA 50%	50	48.5	151	300	202	804	880	6.02	(1.20)	694	1.7	21.0
30	CA 25%	25	48.5	159	429	102	804	880	4.25	(0.80)	691	2.1	20.0
30	CA 50%	50	48.5	152	296	212	804	880	3.96	(0.78)	640	2.6	19.5
30	TU 50%	50	48.5	153	295	215	804	880	3.88	(0.76)	699	1.7	20.0

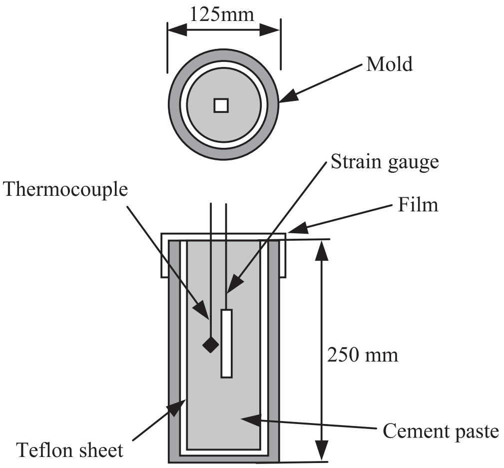

Fig. 1. Measuring the method of strain and temperature of specimen. The strain gauge and the thermocouple were placed vertically. A polytetrafluoroethylene (Teflon) sheet was set between the concrete and the mold to reduce friction so that any initial strain could be measured.

successfully separated with a picric acid methanol solution and the subsequent addition of water.

Ohsawa et al. [22] also measured the degree of hydration of fly ash in coexistence with a $CaSO_4.2H_2O$ and $Ca(OH)_2$ solutions. However, his recent report [23] showed that the picric acid methanol solution is not capable of completely dissolving unreacted cement. Then, he proposed a selective dissolution method using solutions of HCl and Na_2CO_3 [22]. In this study, an HCl and Na_2CO_3 solution was selected for the dissolving solution.

A preweighted centrifuge tube was filled with 1 g of hydrated sample and 30 cm^3 of HCl solution. To accelerate reaction, the centrifuge tube was placed in a 60-°C hot water bath for 15 min. From time to time during this process, the solution was stirred with a glass rod. Then, the liquid phase was extracted centrifugally from the paste using a centrifugal separator at 4000 rpm for 30 s. The liquid phase was decanted without disturbing the solid phase in the bottom of centrifuge tube. Only the solid phase would be used in the next step.

To protect the reaction between the HCl and the Na_2CO_3 solutions, it was necessary to wash out the HCl solution from the sample. The solid phase in the centrifuge tube was filled with hot water, centrifuged again at 4000 rpm for 30 s and decanted. This step was repeated three times. Then the residual specimen was dried at 110 °C for 12 h and weighed.

Following this, the centrifuge tube was filled with 30 cm^3 of Na_2CO_3 solution and placed in an 80 °C hot water bath for 20 min and stirred occasionally. Next, it was again centrifuged at 4000 rpm for 30 s. The supernatant was discarded, and the tube washed in hot water three times to remove the remainder. Next, the tube with the residue sample was dried at 110 °C and weighed.

In these processes, hydrated products such as $Ca(OH)_2$, ettringite and monosulfate were detected using differential thermal analysis (DTA) and thermogravimetric (TG) analysis.

2.3. Determination of autogenous shrinkage

The autogenous shrinkage of concrete was measured according to a method proposed by Nawa et al. [15]. To measure the concrete strain, a thin strain gauge with an elastic modulus of 0.98 N/mm^2 covered with silicon material was used. Fig. 1 shows a schematic figure of a strain gauge and a thermocouple. The strain gauge and the thermocouple were placed vertically in the center of a cylindrical mold 125 mm in diameter and 250 mm in height. A polytetrafluoroethylene (Teflon) sheet was set between the concrete and the mold to reduce friction so that any initial strain could be measured.

The mold was filled with concrete just after mixing. To prevent any evaporation of moisture, the top of the mold was sealed. Then, the samples were kept in a control chamber at a temperature of 20 °C and a humidity of 60±5%. The changes in internal temperature and shrinkage strain were automatically measured and recorded by computer.

3. Results and discussion

3.1. Degree of hydration of fly ash

3.1.1. Verification of method for determining the degree of hydration of fly ash

In the previous study, the effects of the concentration of the HCl and Na_2CO_3 solution on the dissolution of cement and its hydrate were not examined. Thus, this time, the first thing that we examined was the effect of the concentration of the HCl and Na_2CO_3 solution. The results of the experiment are shown in Table 3. From the results, it is obvious that any difference in the amount of sample dissolved by 1.66, 2 and 3 N HCl is negligible. The same result occurred for the 5% and 10% Na_2CO_3 solutions. In this study, we selected a 2 N HCl and 5% Na_2CO_3 for the dissolving solution.

Figs. 2 and 3 illustrate the differential thermal analysis (DTA) and thermo gravimetric (TG) analysis, respectively. To dissolve the component including the Ca ion from the

Table 3
Weights dissolved in selective dissolution method

	1.66 N HCl, 5% Na_2CO_3	2.00 N HCl, 5% Na_2CO_3	3.00 N HCl, 10% Na_2CO_3
Weight dissolved by HCl solution (g)	0.645	0.647	0.654
Weight dissolved by Na_2CO_3 solution (g)	0.036	0.036	0.038
Weight of unreacted fly ash (g)	0.322	0.315	0.312

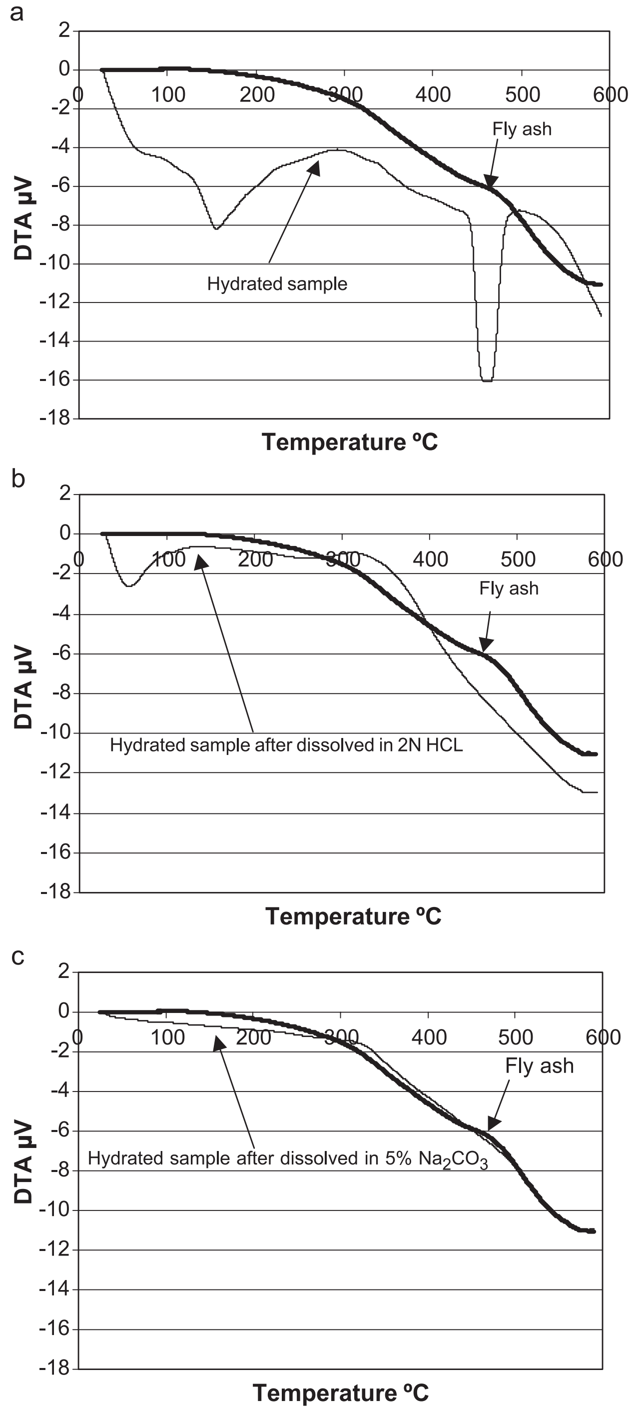

Fig. 2. Differential thermal analysis shows that after the 2 N HCl solution was added, the endotherm peaks at 470, 120 and 160 °C disappeared (Panel b). After the 5% Na_2CO_3 solution was added, the DTA curve became very similar to that of 100% fly ash.

unhydrated OPC and the hydrated products, 2 N HCl was added. Gel composed of SiO_2, Al_2O_3, Fe_2O_3 and unhydrated fly ash was left. After that, 5% of Na_2CO_3 was added to dissolve the SiO_2, Al_2O_3 and Fe_2O_3 gel. Finally, only unreacted fly ash was left.

Fig. 2 shows how the paste that had been hydrated for 28 days and incorporated with 25% fly ash PR/BA containing $Ca(OH)_2$, ettringite and monosulfate corresponded with endotherm peaks at 470,120 and 160 °C, respectively.

After the 2 N HCl solution was added, the endotherm peaks at 470, 120 and 160 °C disappeared. This is due to the dissolution of $Ca(OH)_2$, ettringite and monosulfate. At this stage, a new endotherm peak below 100 °C was observed.

It is well known that SiO_2 gel absorbs moisture very readily. As described previously, 2 N HCl dissolves unhydrated OPC and hydrated products, leaving only the SiO_2, Al_2O_3 and Fe_2O_3 gels and the unhydrated fly ash. The peak below 100 °C of DTA data after the addition of 2 N HCl confirmed that SiO_2 gel existed in this stage.

Next, after the residual sample was filled with a 5% Na_2CO_3 solution, the endotherm peak below 100 °C disappeared, and the DTA curve became very similar to that of 100% fly ash. This result means that the final residual sample was fly ash.

As shown in Fig. 3, after the sample was dissolved with 2 N HCl, the slope of the TG curve resembled that of the 100% fly ash. In the final stage, after the sample was dissolved with 5% Na_2CO_3, the TG curve of the residual extracted sample was almost the same as that of 100% fly ash. Therefore, from both DTA and TG data, it can be concluded that the dissolution method using solutions of 2 N HCl and 5% Na_2CO_3 can determine the degree of hydration of fly ash.

3.1.2. Degree of hydration of fly ash

Table 4 shows the mass of samples after the selective dissolution process of 100% of unhydrated fly ash. These data show that the fly ash was slightly dissolved. This was because some components of the fly ash, such as CaO and MgO, were also dissolved by 2 N HCl. Therefore, this effect should be taken into consideration in the calculation of the degree of hydration of fly ash.

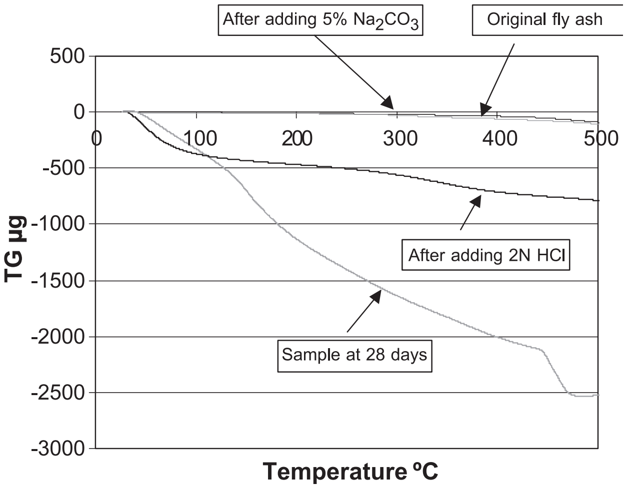

Fig. 3. Thermo gravimetric analysis shows that after the sample was dissolved with 2 N HCl and 5% Na_2CO_3, the TG curve of the residual extracted sample was almost the same as that of 100% fly ash.

Table 4
Residual weight of 100% fly ash

	100% Fly ash		
	PR/BA	TU	CA
Weight of residual fly ash (g)	0.947	0.914	0.913

The degree of hydration of fly ash was calculated for each ignition loss so that it would not include unburned carbon. It was calculated by the following equations.

$$\alpha = 1 - \left[\frac{x_s(1 - Ig_{s'})}{a_1 a_2}\right] \tag{1}$$

$$a_1 = \frac{(1 - Ig_f)R}{(1 - Ig_f)R + (1 - Ig_o)(1 - R)} \tag{2}$$

$$a_2 = \frac{x_f - Ig_F}{1 - Ig_f} \tag{3}$$

In the above, α is the degree of hydration of fly ash. a_1 is the ignitial fraction of fly ash before the dissolution process, a_2 is the residual ignition weight of 100% fly ash after the dissolution process, R is the replacement ratio of fly ash by weight, and x_s and x_f are the weights after the dissolution process of the hydrated sample and unhydrated fly ash, respectively. Ig_f, Ig_F, Ig_o and $Ig_{s'}$ refer to the ignition loss of unhydrated fly ash, unhydrated fly ash after the dissolution process, unhydrated OPC and the hydrated sample after the dissolution process, respectively. In Eq. (1), $x_s(1-Ig_{s'})$ shows the ignition weight of unhydrated fly ash in a hydrated sample after the dissolution process and a_1a_2 shows the ignition weight of unhydrated fly ash in an unhydrated sample after the dissolution process.

The degree of hydration of fly ash with a different replacement ratio is shown in Fig. 4. From this figure, it can be seen that the hydration process of fly ash can be divided into two periods: (1) the accelerated period (before day 56) and (2) the slow period (after day 56).

The period where the degree of hydration is accelerated corresponds to the increase of amount of $Ca(OH)_2$, as shown in Fig. 5. In the slow period (after day 56), the amount of $Ca(OH)_2$ decreased considerably and then became quite constant, resulting in a slow and/or constant degree of hydration of fly ash.

For the degree of hydration of fly ash PR/BA, the sample with 25% PR/BA showed a higher degree of hydration than that of 50% PR/BA. In the accelerated period, the degree of hydration increased gradually, regardless of the replacement ratio of fly ash. The gap in the degree of hydration between 25% PR/BA paste and that of 50% PR/BA paste tended to increase with time. However, for that of fly ash CA, a different tendency was observed. The degree of hydration of 25% CA paste showed a markedly higher value from an early age of 7 days, and after this, the hydration of fly ash did not progress, while that of the 50% CA paste showed an accelerated and slow period. These phenomena can be explained by the size of the particles.

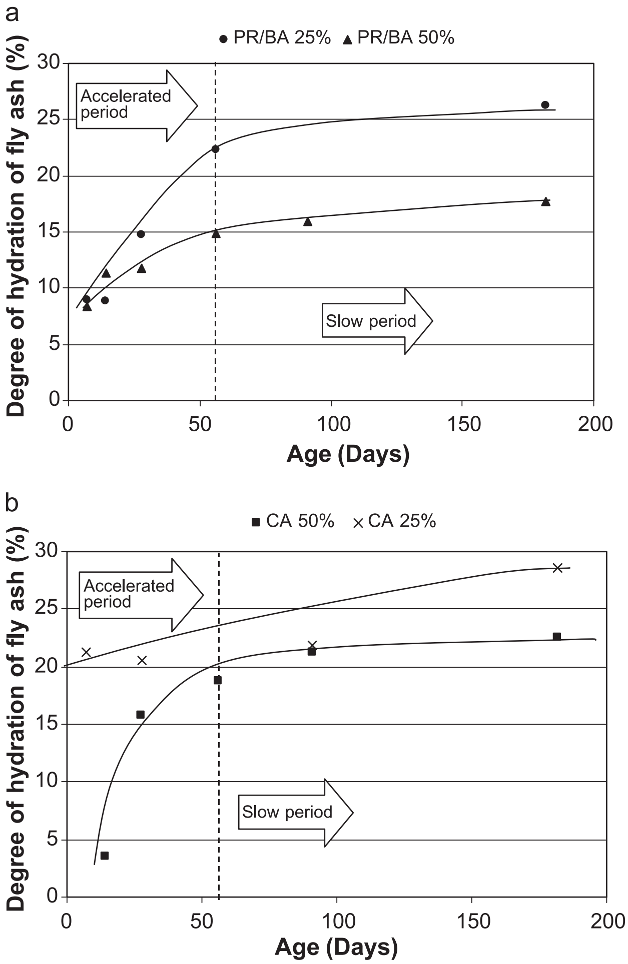

Fig. 4. The degree of hydration of fly ash at different replacement ratios. The hydration process of fly ash can be divided into two periods: (1) the accelerated period (before day 56) and (2) the slow period (after day 56).

From Table 1, the Blaine surface area of fly ash PR/BA was relatively low (279 m^2/kg). This means that the fly ash

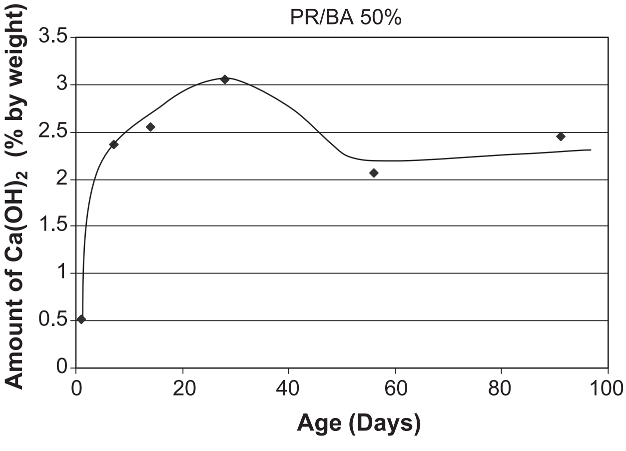

Fig. 5. After day 56, the amount of $Ca(OH)_2$ decreased considerably and then became quite constant, resulting in a slow and/or constant degree of hydration of fly ash.

PR/BA was relatively inert, compared with the OPC and fly ash CA. On the other hand, the Blaine surface area of fly ash CA was quite high (426 m^2/kg). This implies that fly ash CA reacts easier and faster. Particularly, in 25% CA paste, the degree of hydration was high even at an early age.

Fig. 6 shows the degree of hydration of different kinds of fly ash at 50% replacement ratio. Fly ash CA gave the highest degree of hydration, followed by fly ashes PR/BA and TU. The order of degree of hydration of fly ash coincided with the order of the Blaine surface area of fly ash, as shown in Table 1. Thus, this result confirms that the degree of hydration of fly ash is proportional to the particle size of fly ash, indicated by the Blaine surface area.

3.2. Autogenous shrinkage

3.2.1. Results of the experiment

Fig. 7 shows the autogenous shrinkage as age increases. As shown in Fig. 7a, the autogenous shrinkage increased when the replacement of fly ash was 25%. However, when the replacement ratio reached 50%, the autogenous shrinkage had become remarkably small. The rate of autogenous shrinkage strongly changed between 0 and 12 h, but changed slowly after 12 h. From Fig. 7, the behavior of autogenous shrinkage can be separated into four stages as follows.

3.2.1.1. Stage 1: Start of sedimentation. After the concrete was laid, the solid fractions instantly started to move downward under the gravity force, and then some of the water rose or bled to the surface. The change in the volume of the concrete was very small in this stage. Several ions rapidly dissolved from cement particles, corresponding to the preinduction period in the hydration process of OPC. A small quantity of hydrated product precipitated in the region of the surface of the cement particles and in the paste solution. The reaction tended to slow down due to the deposition of a layer of hydration products around the cement particle surface [24]. It seems that the hydration process in this stage did not have much effect on the shrinkage.

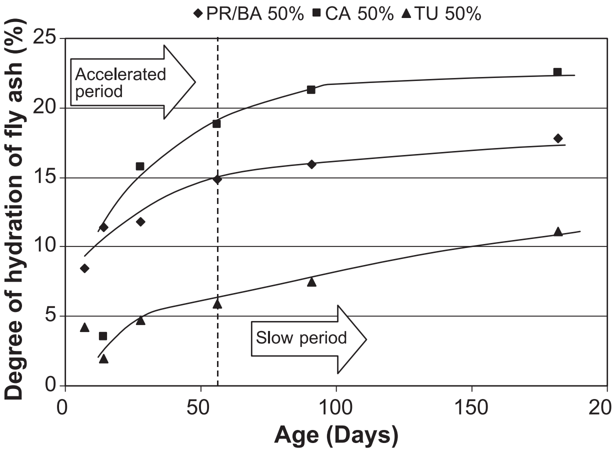

Fig. 6. The comparison of degree of hydration for different kinds of fly ash. Fly ash CA gave the highest degree of hydration, followed by fly ash PR/BA and fly ash TU.

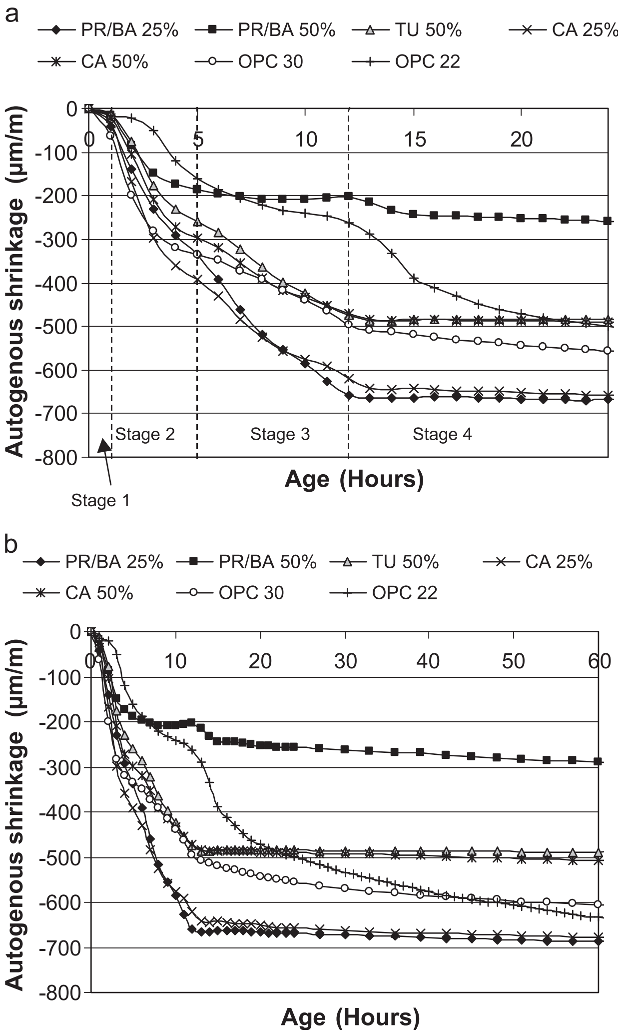

Fig. 7. Shows that autogenous shrinkage increased when the replacement of fly ash was 25%. However, when the replacement ratio reached 50%, the autogenous shrinkage had become remarkably small.

3.2.1.2. Stage 2: Accelerated sedimentation. This stage occurred almost simultaneously with the induction period in the hydration process, in which the hydration of all the clinker minerals progressed very slowly. The change of temperature in Fig. 8 shows that the temperature in this period was quite constant. Thus, it seems that its large shrinkage does not derive from hydration but from the rapid sedimentation of particles.

3.2.1.3. Stage 3: Autogenous shrinkage due to hydration of OPC. This period corresponds to the acceleration stage in the hydration process of OPC (3 to 12 h after mixing). When the hydration rate increased, the temperature of the concrete sample also increased. As the cement hydrated, the hydration products formed around the cement particles and filled up the water-filled spaces between the solid

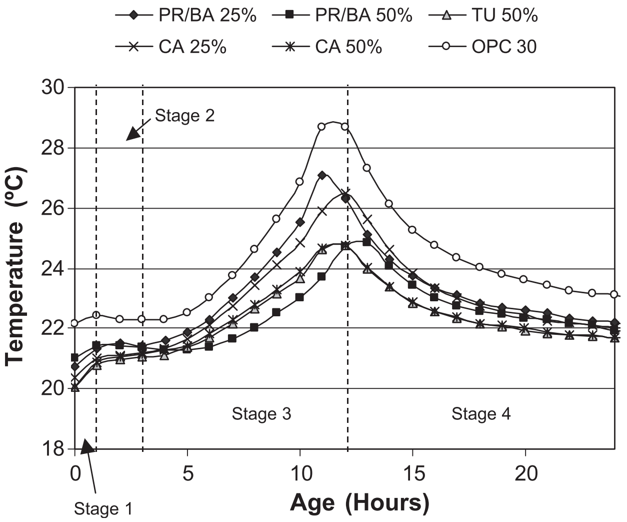

Fig. 8. Temperature inside the sample.

particles in the concrete. All the cement particles had become bounded by their hydrates. The water between the surface of the cement particles and/or their hydrates held small capillaries and formed such menisci. The water in the small capillaries exerted hydrostatic tension. As a result, this capillary pressure reduced the distance between the solid concrete particles, making the concrete shrink [2].

Real autogenous shrinkage started to develop after the initial setting. Sedimentation of particles still continued in this stage, but the effect tended to become less important as the rate of cement hydration increased. At the end of this stage, the temperature of the samples had reached the maximum.

3.2.1.4. Stage 4: Post autogenous shrinkage. This stage started when the temperature of the sample started to decline, corresponding to the post acceleration period in the hydration process. The temperature decreased gradually, as the amount of still nonreacted cement declined and the rate of the hydration process of cement became diffusion controlled [24]. The particles had become fixed to each other by the hydrated product, thus, the effect of particle settlement was negligible. The autogenous shrinkage up to 50 and 400 days is shown in Fig. 9. At day 5, the fly ash–OPC sample showed some kind of expansion behavior. The autogenous shrinkage of the sample with 25% fly ash was no different from that of the OPC sample. This means that 25% fly ash was not enough to mitigate the autogenous shrinkage.

3.2.2. Discussion

In general, concrete prepared with a lower water–binder ratio shows a higher autogenous shrinkage. However, the results of the experiment in this study showed that at an early age, the autogenous shrinkage of OPC concrete with water–cement ratio (W/C) 0.30 was higher than that of OPC concrete with W/C 0.22. This could be explained by the effect of the superplasticizer.

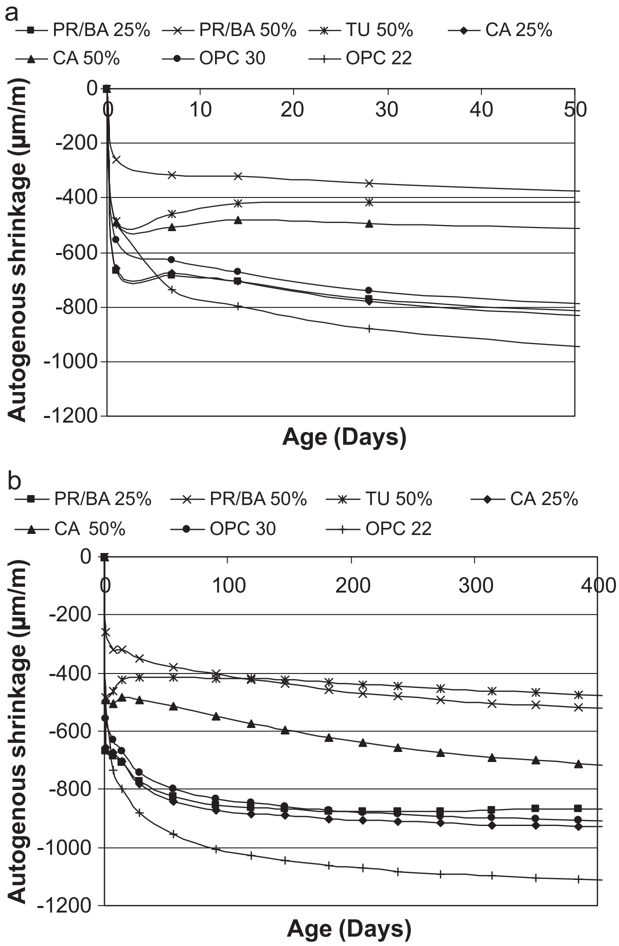

Fig. 9. Autogenous shrinkage up to 400 days.

It is well known that after superplasticizer is added, it adsorbs on the particle surface. The main chain of polymer is adsorbed on the powder surface. After that, the graft chains stretch out. The particles are covered with a macromolecular-adsorbed layer. Repulsive force is induced when such layers overlap so that the particles are stably dispersed [25–27]. However, the superplasticizer delays the hydration

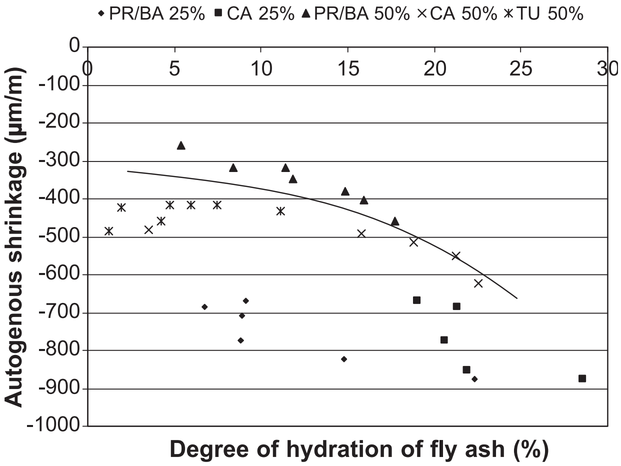

Fig. 10. Autogenous shrinkage and degree of hydration of fly ash.

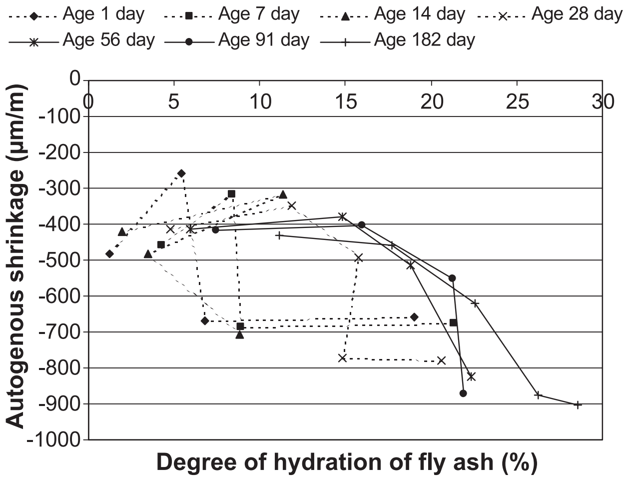

Fig. 11. Autogenous shrinkage and degree of hydration of fly ash considered at the same age.

of OPC. When a large amount of superplasticizer is used, the hydration is significantly delayed, accordingly providing a delay in autogenous shrinkage.

In as much as the mix proportion of the concrete in this experiment was designed to have the same flow ability, the amount of superplasticizer was adjusted to suit the given slump flow. The OPC concrete W/C 0.22 sample contained a larger amount of superplasticizer than did the OPC concrete with W/C 0.30. Thus, OPC concrete with W/C 0.22 showed a lower autogenous shrinkage at an early age. However, over a long period, when the retarding effect of the superplasticizer became negligible, the autogenous shrinkage of OPC concrete with W/C 0.22 became higher than that of OPC concrete with W/C 0.30.

Fig. 10 illustrates the relationship of autogenous shrinkage and the degree of hydration of fly ash. It appears that autogenous shrinkage increased as the degree of hydration of fly ash increased. For concrete mixed with 50% of fly ash, there was a relation between autogenous shrinkage and the degree of hydration of fly ash. However, for the sample with 25% of fly ash, no distinct relation could be found. Therefore, it might be concluded that, for the sample with 25% of fly ash, autogenous shrinkage was superiorly affected by the hydration of the OPC.

Fig. 11 shows the relation between autogenous shrinkage and the degree of hydration of fly ash at different ages, regardless of the kinds of fly ash. In early ages, there is no relation. This indicates that only a degree of hydration of fly ash is insufficient to explain the mechanism of autogenous shrinkage.

Many researchers reported that the autogenous shrinkage of OPC mixes was higher than that of high-belite Portland cement mixtures [12,15,28]. One reason given was the lower amount of C_3A or lower reactive Al_2O_3 in high-belite Portland cement [12]. It might be possible that the same phenomena occurs in fly ash–cement mixes.

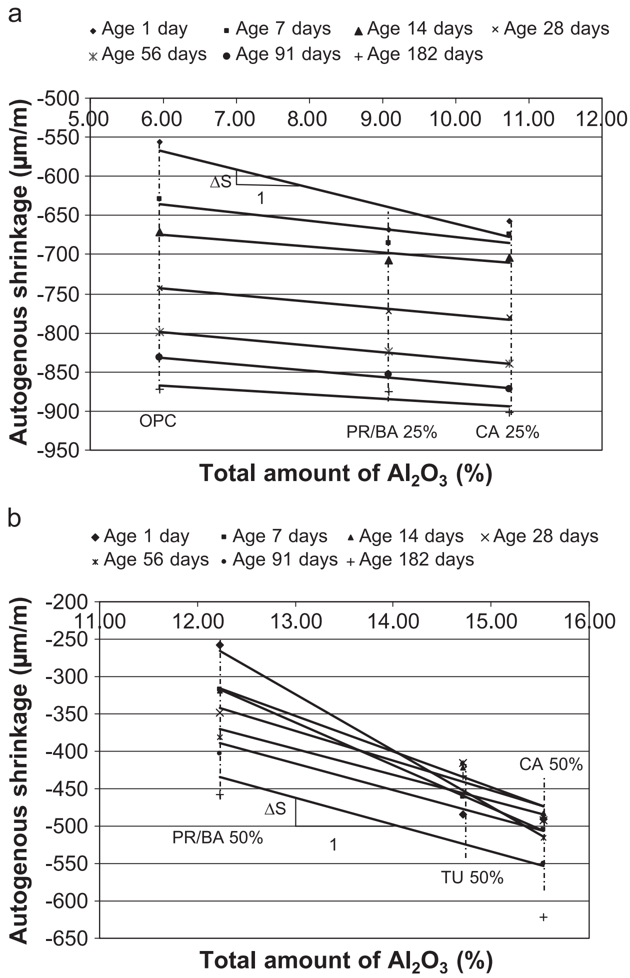

Fig. 12. Autogenous shrinkage and total amount of Al_2O_3.

Berry et al. [19] reported that during 2 to 5 h after mixing, the amount of ettringite in fly ash–cement mixes was higher than that in the OPC mixes. The chemical reaction of Al_2O_3 of fly ash to produce ettringite is shown by the following equation [29]:

$$Al_2O_3 + 3Ca(OH)_2 + 3CaSO_4 + 29H_2O = 3CaO.Al_2O_3.3CaSO_4.32H_2O \qquad (4)$$

This equation shows that the reaction that produces ettringite consumes much water. As a result, this might cause the pores to empty. Accordingly, the autogenous shrinkage becomes larger.

Table 5
The amount of total Al_2O_3

	OPC	PR/BA 25%	CA 25%	PR/BA 50%	CA 50%	TU 50%
Total Al_2O_3 (%)	5.95	9.09	10.74	12.23	15.53	14.71

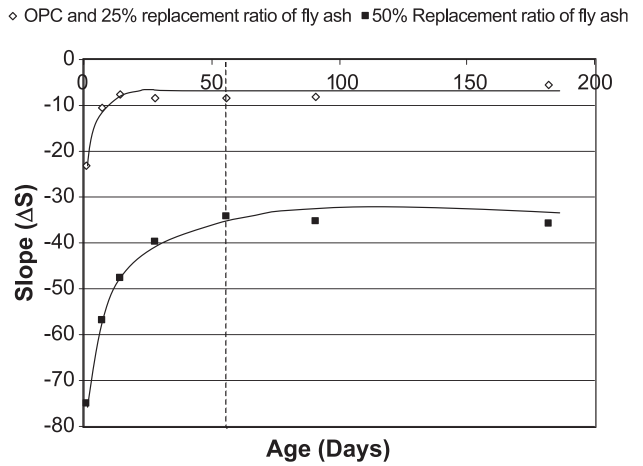

Fig. 13. Slope (ΔS) of the curve in Fig. 12 at different ages. As the age of the specimens increases, the ΔS value reduces conversely. When the sample age increases, the effect of Al_2O_3 may be smaller; after an age of 56 days, ΔS value was quite constant.

Moreover, Justnes et al. [30] reported that in an OPC mixture, the total volume change of C_3A reaction in Eq. (4) was reduced by 0.273 cm^3/g of C_3A when it reacted with water and calcium sulfate to produce ettringite. Therefore, the solid fraction might shrink due to the reaction, to produce ettringite at early ages.

However, it should be noted that the volume change calculated by Justnes [30] might not include the spaces between the crystals of ettringite, the shape of which is needle like. When a large quantity of ettringite crystals are produced, it is quite likely that they are not parallel to each other. At this time, it is possible that spaces form between the ettringite crystals. At very early ages, cement mixes might shrink, but after a large quantity of ettringite is produced, the cement mixes might exhibit expansion. In this study, expansion was noticed at around day 5, as shown in Fig. 9a.

Table 5 shows the total amount of Al_2O_3 content, the calculation based on the replacement ratio and the amount of Al_2O_3 in the fly ash and OPC. The total amount of Al_2O_3 varied depending on the replacement ratio and amount of Al_2O_3 in the fly ash.

Fig. 12 shows the relation between autogenous shrinkage and the total amount of Al_2O_3 at different ages. The slope (ΔS) of the curve in Fig. 12 indicates the significant effect of Al_2O_3. It seems that the effect of Al_2O_3 varies with time. The large ΔS value implies that Al_2O_3 had a large effect on the autogenous shrinkage. The change of slope (ΔS) in Fig. 12 is illustrated as a function of age in Fig. 13. This figure shows that, as the age of the specimens increases, the ΔS value reduces conversely. This implies that when the sample age increases, the effect of Al_2O_3 may be smaller; after an age of 56 days, ΔS value was quite constant.

After day 56, the effect of Al_2O_3 may become less important. It is possible that autogenous shrinkage mainly depends on the degree of hydration of fly ash in the long term. A corresponding result can be found in Fig. 11. From day 56, the relation of autogenous shrinkage and the degree of hydration of fly ash started to show a tendency. Regardless of the kinds of fly ash, autogenous shrinkage tended to increase with the increase in the degree of hydration of fly ash.

In addition, in the paste with 50% replacement of fly ash, the degree of hydration of fly ash was considerably low. Thus, the proportion of unhydrated fly ash was quite high. The unreacted fly ash may act like a microaggregate. Because the unhydrated fly ash cannot shrink, the total autogenous shrinkage can be reduced.

4. Conclusions

This study investigated the degree of hydration of fly ash and then used the degree of hydration of fly ash and its chemical component to explain the mechanism of autogenous shrinkage. Based on the test results obtained in this research, the following conclusions can be drawn.

4.1. The degree of hydration of fly ash

The dissolution method with the 2 N HCl and 5% Na_2CO_3 solutions is suitable for measuring the degree of hydration of fly ash. The degree of hydration of fly ash is proportional to the particle size of the fly ash. The hydration mechanism of fly ash can be divided into two periods: (1) the accelerated period (before day 56) and (2) the slow period (after day 56).

4.2. Autogenous shrinkage

The process of autogenous shrinkage could be divided into four stages. The shrinkage in Stages 1 and 2 mainly resulted from the movement of particles downward due to gravity formation. In Stage 3, autogenous shrinkage tended to depend on the hydration reaction of OPC and the reaction of Al_2O_3 to form ettringite. In Stage 4, autogenous shrinkage tended to slow down. After day 56, the effect of Al_2O_3 may become less important and autogenous shrinkage may depend mainly on the degree of hydration of fly ash.

References

[1] T.C. Powers, Absorption of water by Portland cement paste during hardening process, Ind. Eng. Chem. 27 (7) (1935) 790–794.

[2] F.H. Wittmann, On the action of capillary pressure in fresh concrete, Cem. Concr. Res. 6 (1) (1976) 49–56.

[3] E. Tazawa, S. Miyazawa, Autogenous shrinkage of concrete and its importance in concrete technology, in: Z.P. Bazant, L. Carol (Eds.), Proceedings of the Fifth International RILEM Symposium on Creep and Shrinkage of Concrete, E and FN Spon, London, 1993, pp. 159–168.

[4] E.J. Sellevold, The function of condensed silica fume in high strength concrete, FIP Notes 4 (1987) 11–14.

[5] H. Justnes, B. Reyniers, D. Van Loo, E.J. Sellevold, An evaluation of method of measuring chemical shrinkage of cementitious paste, Nord. Concr. Res. 14 (1) (1994) 45–61.

[6] E. Tazawa, S. Miyazawa, K. Shigekawa, Macroscopic shrinkage of hardening cement paste due to hydration, CAJ Proc. Cem. Concr. 45 (1991) 528.

[7] T.C. Holland, A. Krysa, M.D. Luther, T.C. Liu, Use of silica fume concrete to repair abrasion–erosion damage in the Kinzua Dam Stilling Basin, 2nd CANMET/ACI Int. Conf. ACI. On Fly Ash, Silica Fume, Slag and Natural Pozzolans in Concrete, vol. SP-91, 1986, pp. 841–863.

[8] B. Persson, Self-desiccation and its importance in concrete technology, Mater. Struct. 30 (1997) 293–305.

[9] Y.W. Chan, C.Y. Liu, Y.S. Lu, Effect of slag and fly ash on the autogenous shrinkage of high performance concrete, in: E. Tazawa (Ed.), Proceedings of the International Workshop on Autogenous Shrinkage of Concrete, JCI, Hiroshima, Japan, 1998, pp. 221–228.

[10] S. Tangtermsirikul, Effect of chemical composition and particle size of fly ash on autogenous shrinkage of paste, in: E. Tazawa (Ed.), Proceedings of the International Workshop on Autogenous Shrinkage of Concrete, JCI, Hiroshima, Japan, 1998, pp. 175–186.

[11] K. Wang, S.P. Shah, P. Phuaksuk, Plastic shrinkage cracking in concrete materials—influence of fly ash and fibers, ACI Mater. J. 98-M49 (2001) 458–464.

[12] K.B. Park, T. Noguchi, F. Tomosawa, A study on the hydration ratio and autogenous shrinkage of cement paste, in: E. Tazawa (Ed.), Proceedings of the International Workshop on Autogenous Shrinkage of Concrete, JCI, Hiroshima, Japan, 1998, pp. 299–308.

[13] P. Lura, O.M. Jensen, K. van Breugel, Autogenous shrinkage in high-performance cement paste: an evaluation of basic mechanisms, Cem. Concr. Res. 33 (2) (2003) 223–232.

[14] A. Princigallo, P. Lura, K. van Breugel, G. Levita, Early development of properties in a cement paste: a numerical and experimental study, Cem. Concr. Res. 33 (7) (2003) 1013–1020.

[15] T. Nawa, T. Horita, H. Ohnuma, A study on measurement system for autogenous shrinkage of cement mixes, in: R.K. Dhir, M.D. Newlands, T.A. Harrison (Eds.), Concrete Floors and Slabs, Thomas Telford, Scotland, 2002, pp. 281–290.

[16] C.S. Poon, L. Lam, Y.L. Wong, A study on high strength concrete prepared with large volumes of low calcium fly ash, Cem. Concr. Res. 30 (3) (2000) 447–455.

[17] L. Lam, Y.L. Wong, C.S. Poon, Degree of hydration and gel/space ratio of high-volume fly ash/cement systems, Cem. Concr. Res. 30 (5) (2000) 747–756.

[18] Y.M. Zhang, W. Sun, H.D. Yan, Hydration of high-volume fly ash cement pastes, Cem. Concr. Res. 22 (6) (2000) 445–452.

[19] E.E. Berry, R.T. Hemmings, B.J. Cornelius, Mechanisms of hydration reactions in high volume fly ash pastes and mortars, Cem. Concr. Compos. 12 (1990) 253–261.

[20] A.M. Neville, Properties of Concrete, 3rd ed., ELBS with Longman, London, 1981, pp. 257–279.

[21] S. Takashima, Sem. Gijutsu Nempo, 11, 188 (1957) m JCEA Rev. 11th Gen. Mtg., 45 (1957) (in Japanese).

[22] S. Ohsawa, K. Asaga, S. Goto, M. Daimon, Quantitative determination of fly ash in the hydrated fly ash–$CaSO_4.2H_2O$-$Ca(OH)_2$ system, Cem. Concr. Res. 15 (1985) 357–366.

[23] S. Ohsawa, E. Sakai, M. Daimon, Reaction ratio of fly ash in the hydration of fly ash–cement system, Sci. Technol. Cem. Concr. 53 (1999) 96–101 (in Japanese).

[24] Peter C. Hewlett, Mechanism of hydration, Lea's, chemistry of cement and concrete, fourth ed., Reed Educational and Professional Publishing, Oxford, 1998, pp. 265–268.

[25] P. Termkhajornkit, T. Nawa, H. Ohnuma, Effects of properties of fly ash on fluidity of paste, Sci. Technol. Cem. Concr. 55 (2001) 163–169.

[26] P. Termkhajornkit, Role of Fly Ash on The Fluidity of Paste, A master thesis submitted to Hokkaido University Graduate School of Engineering, (2002) pp. 35.

[27] M. Kinoshita, T. Nawa, M. Iida, and H. Ichiboji, Effect of Chemical Structure on Fluidizing Mechanism of Concrete Superplasticizer Containing Polyethylene Oxide Graft Chains, ACI SP195-11, (2000)163–180.

[28] E. Tazawa, S. Miyazawa, Influence of constitutes and composition on autogenous shrinkage of cementitious materials, Mag. Concr. Res. 49 (178) (1997) 15–22.

[29] Xinghua Fu, Zhi Wang, Wenhong Tao, Chunxia Yang, Wenping Hou, Youjun Dong, Xuequan Wu, Studies on blended cement with a large amount of fly ash, Cem. Concr. Res. 32 (7) (2002) 1153–1159.

[30] H. Justnes, T. Hammer, B. Ardoullie, E. Hendrix, D. Van Gemert, K. Overmeer, E.J. Sellevold, The influence of cement characteristics on chemical shrinkage, in: E. Tazawa (Ed.), Proceedings of the International Workshop on Autogenous Shrinkage of Concrete, JCI, Hiroshima, Japan, 1998, pp. 221–228.